IJBPAS, February, 2023, 12(2): 724-737

ISSN: 2277–4998

International Journal of Biology, Pharmacy and Allied Sciences (IJBPAS)

'A Bridge Between Laboratory and Reader'

www.ijbpas.com

# ANTIUROLITHIATIC ACTIVITY OF BIOGENICALLY SYNTHESIZED SILVER NANOPARTICLES USING THE STEM BARK EXTRACT OF *Hybanthus enneaspermus* (l) f. Muell

**KANMANI R[1*], DEVIKA S[1], KAVITHA M[1] AND SHENBAGAM K[2]**

**1:** PG & Research Department of Chemistry, Holy Cross College (Autonomous), Tiruchirappalli

**2:** PG Department of Chemistry, Cauvery College for Women (Autonomous), Tiruchirappalli, Affiliated to Bharathidasan University, Tiruchirappalli

***Corresponding Author: Dr. Kanmani R: E Mail: kanmanivincy@gmail.com**

**Received 29th March 2022; Revised 29th April 2022; Accepted 19th July 2022; Available online 1st Feb. 2023**

https://doi.org/10.31032/IJBPAS/2023/12.2.6841

## ABSTRACT

Nanoparticles are often made using a variety of chemical processes that are not environmentally friendly. As a result, in this work, we used green synthesis of silver nanoparticles (Ag Nps) owing to its capabilities, environmentally friendly progress, and low cost. The silver nanoparticles were created with of *Hybanthus enneaspermus* ethanolic stem bark extract. Various spectroscopic methods, such as Scanning electron microscopy (SEM), Fourier transform infrared spectroscopy (FITR), Energy dispersive X-ray spectroscopy (EDX), X-ray Diffraction (XRD), and UV- Visible spectroscopy were used to evaluate the produced silver nanoparticles. The face-centered cubic crystal structure of the produced Ag Nps is validated by the XRD data. The antiurolithiatic activity of produced Ag Nps was examined through a single gel diffusion approach. Based on the results, it was determined that the stem bark of *Hybanthus enneaspermusm* facilitated silver nanoparticles had a higher proportion of inhibition towards struvite crystals.

**Keywords: *Hybanthus enneaspermus,* Phytochemical Analysis, Quantitative Estimation, Silver nanoparticles, Antiurolithiatic activity**

## INTRODUCTION

Environmentally friendly 'green' methods in chemistry and chemical industries are often more prominent and highly required as a consequence of global

difficulties related to environmental issues **[1]**. Silver is amongst the most exploited nanomaterials, with 500 tons of silver nanoparticles produced every year **[2]**, and this figure is anticipated to increase in the coming years. It has been recognized to have powerful bactericidal and inhibitory effects, as well as anti-angiogenesis, and anti-fungal, anti-inflammatory activities **[3, 4]**, in addition to its significant importance in the area of medicine, high sensitivity biomolecular detection, biosensors, and catalysis. There are a variety of methods offered for the production of Ag Nps, such as sol gel, ion sputtering, chemical reduction, and so on **[5-8]**. However, most of those nanomaterials fabrication techniques require the usage of high energy demands or dangerous chemicals, which are complicated and wasteful cleansings **[9]**. As a result, regardless of the approach used, chemical pollutions will always occur during the syntheses operations or in possible uses, with related constraints. Nonetheless, one cannot dispute its ever-expanding uses in everyday life. For example, "The Noble Silver Nanoparticles" are aiming for cutting-edge utility in each element of science and technology, along with the medicinal professions; consequently, they cannot be ignored solely owing to its origin of creation. As a result, it has become a duty to promote an alternative synthetic approach, which is not only cost efficient but also ecologically benign. In terms of aesthetics, green syntheses are establishing itself as major procedures and demonstrating its possibility at the forefront. Strategies for producing nanostructures utilizing naturally available substances for example plant extracts, sugars, microorganisms and chitosan (biodegradable polymer) as capping and reducing agents may be appealing for nanotechnology **[9-11]**. Greener nanoparticle production gives an advantage over former approaches since it is cost-effective, easy, reasonably repeatable, environmentally friendly, one step, and it eventually resulted in more stable materials **[12]**. Furthermore, microorganisms may also be utilized to create nanomaterials, however the rate of synthesis is slower than that of plant-mediated synthesis **[9]**. However, the promise of plant species as a feedstock for this reason remains largely untapped. Plant extracts of *Ziziphora tenuior* **[13]**, *marigold* flower **[7]**, *Abutilon indicum* **[14]**, *Erythrina indica* **[8]**, *Solanum tricobatum* **[15]**, beet root **[5]**, *Ocimum tenuiflorum* **[16]**, *mangosteen* **[4]**, *Spirogyra varians* **[17]**, *Melia dubia* **[14]**, olive [18], *Acalypha indica* **[19]** and particles of *Sesuvium portulacastrum*, with nanoparticle sizes ranging from 5 to 20 nm [20], have been described in the literature as a substrate for the manufacture of Ag

Nps as a substitute for traditional procedures.

Urolithiasis is a disorder in which urinary calculi occur or are found somewhere else in the urinary tracts, or the approach of stone production in the ureter, kidney or bladder **[21]**. It is ranked as the third most frequent urinary tract infection **[22]**. The majority of the public and medical professionals are searching for new medical interventions since many current pharmaceuticals have side effects **[23]**, which is claimed to be a superior method leveraging nanotechnology advances in medical **[24]**. As a result, the current work emphases on the synthesis and characterization of nanosize Ag, where Ag Nps were synthesized from *Hybanthus enneaspermus* stem bark extract as an Ag reduction agent and its biological features as antiurolithitaic activity were further examined.

## MATERIALS AND METHODS

### Preparation of stem bark extract of *Hybanthus enneaspermus*

The *Hybanthus enneaspermus* stem bark was collected from the Perambalur district and cut into a small size of pieces. The collected plant stem bark is totally washed with tap water and dried under the sun shadow place. Using the mortar and pestle to grind the stem bark into powdered and then stored. The extract was prepared by cold percolation method. The extract is prepared using ethanolic solution. About 20g of stem bark powder sample in a beaker and 40ml of ethanol is added and it is soaked for 24 hours.

### Phytochemical screening

The qualitative analysis of stem bark of *Hybanthus enneaspermus* ethanolic extract was done by standard tests and it was used to identify the various phytoconstituents present in the sample.

### Quantitative Estimation of phytochemical constituents present in plants

Quantitative estimation of phytochemical constituents of stem bark of *hybanthus enneaspermus* was carried out by standard methods. The results were represented in mg/g.

### Silver nanoparticle synthesis

A 100 ml standard flask was filled with a 5mm $AgNO_3$ solution. Through constant stirring, 2.5ml of material is poured to 50ml of 5mm $AgNO_3$ solution. In an ambient environment, the combination is reacted, and silver is reduced in $Ag^0$ ion. Color changes were seen after a few minutes. As in, from clear white to dark brown. In other words, the color shift directs the creation of Ag Nps. The creation of Ag Nps was verified somewhat by UV-spectral analysis.

### Characterization of silver nanoparticles

Characterization procedures are utilized to govern the particle wavelength

and functional group characteristics of produced silver nanoparticles. The bonded functional group was detected using FTIR and UV-Visible spectra, and the crystalline nature, shape, size, and elemental composition were characterized using XRD, SEM, and EDAX.

**The growth of struvite crystals and its characterization**

The single diffusion reaction method was engaged. The crystal growth of sample is formed when 0.5M ammonium dihydrogen phosphate (ADP) is used and is taken in a test tube. Sodium meta silicate solution added with the side of test tube and the density of 1.04g/cm$^3$ and it contains the pH level is 9.4. Then the mixture pH level is maintained at range of 6. The gel is formed and closed with airtight stoppers and the gel is undisturbed for about 4 to 5 days. After few days the gelation process, the 1 molarity of magnesium acetate was added in gel test tubes without disturbing gel. After the added solution, it kept at room temperature and carried out the full experiment with the temperature at 37°C. The structure and growth of the crystals were confirmed through FTIR. This method is to achieve the pureness and appropriate development of crystals.

**The classification of struvite crystals growth with different additive solution**

Using the sol gel method, the growth of struvite crystal was studied by the stem bark of *Hybanthus enneaspermus* extract. The growth of struvite crystals was studied by different concentration such as 1, 2, 3, 4 and 5% is represented in **Table 1**. The different concentration of the created silver nanoparticles is added in equal amount of supernatant solution and development of the crystals were restrained depending on their average weight.

I% inhibition was premeditated based on the formulae.

**I % = [(TSI-TAI)] / TSI X 100**

TSI are denotes the crystal numbers without inhibitors

TAI is denotes the crystal number after the addition of inhibitors.

**Table 1: Sol gel contains supernatant solution for the growth of struvite crystals Supernatant solution (control and composition of synthesized silver measures) nanoparticles**

| | |
|---|---|
| A (Control) | 10ml of 1M magnesium acetate |
| B (Control + distilled water) | 5ml of 1M magnesium acetate + 5ml of distilled water |
| C (Control + methanol) | 5ml of 1M magnesium acetate + 5ml of Ethanol) |
| D (1% synthesized Ag Nps) | 5ml of 1 M Magensium acetate + 5ml of 1% synthesized Ag Nps |
| E (2% synthesized Ag Nps) | 5ml of 1M Magnesium acetate + 5 ml of 2% synthesized Ag Nps |
| F (3% synthesized Ag Nps) | 5ml of 1M Magnesium acetate + 5ml of 3% synthesized Ag Nps |
| G (4% synthesized Ag Nps) | 5ml of 1M Magnesium acetate + 5ml of 4% synthesized Ag Nps |
| H (5% synthesized Ag Nps) | 5ml of 1M Magnesium acetate + 5ml of 5% synthesized Ag Nps |

## RESULTS AND DISCUSSION

The phytochemical screening results were represented in **Table 2**. It shows the stem bark of *Hybanthus enneaspermus* extract contains terpenoids, flavanoids, tannins, alkaloids, steroids, coumarins, emodins, anthroquinones, xanthoproteins, phenols, saponins, glycosides, phlobatannins, anthocyanins, carbohydrates, lawanthocyanins and cardicglycosides **(Figure 2)**. The phytochemical constitutents all have medicinal and physiological activities.

The phytoconstituents found in Hybanthus enneaspermus stem bark extract in various amounts were described based on qualitative investigation. Saponins were the phytoconstituents found in the greatest proportion in plants, preceded with flavonoids, phenols, terpenoids, tannin, and alkaloids **(Table 3)**. The weight of phytoconstituents are shown in **Figure 3**, such as Flavonoids (0.004mg/g), Tannins (0.017 mg/g), saponins (0.018mg/g), phenols (0.005mg/g) and Terpenoids (0.004mg/g) **(Figure 3)**.

These results are used to study the antioxidant activity. The phenolic compounds most involved in the anti-tumor and anti-oxidant activity. The flavonoids showed the major role of cytotoxicity activity and free radical scavenging activity.

### UV- Visible spectroscopy

The development of Ag Nps with the stem bark ethanolic extract of *Hybanthus enneaspermus* were confirmed by Ultra violet visible spectroscopy. Using the UV visible spectroscopy, the color change is observed in the sample. The color is changed from colorless to dark brown color and it's indicated the presence of silver nanoparticles. The color range absorbed by UV- Visible spectroscopy and the range is 447nm **(Figure 4)**.

### FT-IR spectroscopy analysis

This approach is utilized to investigate the functional in our material that is accountable for the creation of Ag Nps **(Figure 5)**. The FTIR spectrum frequencies of the produced Ag Nps are shown in **Table 4**. The inclusion of flavanoids and phenols is strongly suggested; these compounds are mainly accountable for the creation of Ag Nps. Based on the FT IR spectra, it was determined that the extract included carboxyl and hydroxyl groups, which operate as stabilizing and reducing agents, respectively, and that the presence of phenolic groups could serve as a capping agent.

### Scanning electron microscopy

Scanning electron microscopy revealed the surface morphology of silver nanoparticles. The SEM picture of the produced silver nanoparticles revealed their cubic and spherical form. **Figure 6** depicts

the presence of generated silver nanoparticles in the region between 127.4nm and 90.70nm.

**EDX analysis**

The EDX spectrometer is used to identify the components contained in the produced silver nanoparticles. For manufactured silver nanoparticles, EDX revealed an extra oxygen signal. The surface of silver nanoparticles is connected to the biomolecules in this way. **Figure 7** depicts EDX spectra. The silver content of generated silver nanoparticles is 60.34 percent **(Table 5)**.

**X- Ray diffraction (XRD)**

The crystallinity of silver nanoparticles is determined via X-ray diffraction. The XRD diffraction values of produced silver nanoparticles have been in the range of 2θ for 38.1495, 45.6498, 67.0102, 78.2357, and 78.4218. The corresponding peaks are 38.1495 and 45.6498. These diffraction facts are (111) and (200), respectively. The diffraction patterns for synthesised silver nanoparticles (111), (200), (220), and (221) were observed (311). According to this, reflection indicated the face-centered cubic structure for produced silver nanoparticles (JCPDS, Files No: 04-0783). The graph might be found among the unassigned peaks. This is because the extract includes additional phytochemicals. The phytochemicals cover the surface of the nanoparticles **(Figure 8)**.

***In-vitro* Antiurolithiatic activity**

The shape of the collected crystal was observed from the administration of the inhibitor on a regular basis for up to 7 days, as shown in **Figure 10**. The size of the crystal was progressively reduced through increasing the quantity of Ag Nps, as shown in **Figure 11**. According to the findings, the average weight of the struvite crystals steadily drops from 2.46 g to 0.25 g. The highest inhibitory performance was found to be 89.8 percent.

From this study, realized that the distilled water has no inhibitory activity with respect to crystal growth. In case of synthesized silver nanoparticles in stem bark extract of *Hybanthus enneaspermus* revealed the inhibitory activity due to bioorganic molecules and phytochemical consists present in stem bark of *Hybanthus enneaspermus* **(Table 6, Figure 9)**.

**FT-IR assessment of harvested crystals**

**Table 7** shows the FT-IR spectra of struvite crystals produced in the existence and exclusion of the plant sample. According to the findings, the shift in the FT-IR bands identifies the existence of effective functional groups, and the rate of production of struvite crystals slows owing to the inhibitory activity of *Hybanthus enneaspermus* assisted Ag Nps.

**Table 2: Qualitative analysis of stem bark of *hybanthus enneaspermus***

| S. No. | Test for | Observation | Result |
|---|---|---|---|
| 1 | Terpenoids | Reddish brown | +++ |
| 2 | Flavanoids | Yellow color | +++ |
| 3 | Saponins | Blue color | ++ |
| 4 | Tannins | Brownish green | +++ |
| 5 | Alkaloids | Yellow color | +++ |
| 6 | Steroids | Reddish brown | +++ |
| 7 | Glycosides | Violet, blue | ++ |
| 8 | Phlobatanins | Red precipitate | ++ |
| 9 | Proteins | White | _ |
| 10 | Coumarins | Yellow | +++ |
| 11 | Emodins | Red | +++ |
| 12 | Anthroquinones | Pink, Violet | +++ |
| 13 | Anthocyanins | Pinkish red, Blusih violet | ++ |
| 14 | Carbohydrates | Reddish pink | + |
| 15 | Lawanthocyanins | Red | + |
| 16 | Cardiacglycosides | Brown ring / Violet | + |
| 17 | Xanthoproteins | Blue /black | +++ |
| 18 | Phenols | Reddish / orange | +++ |

**+ - Trace ++ - Moderate +++ - Strong A – Absence**

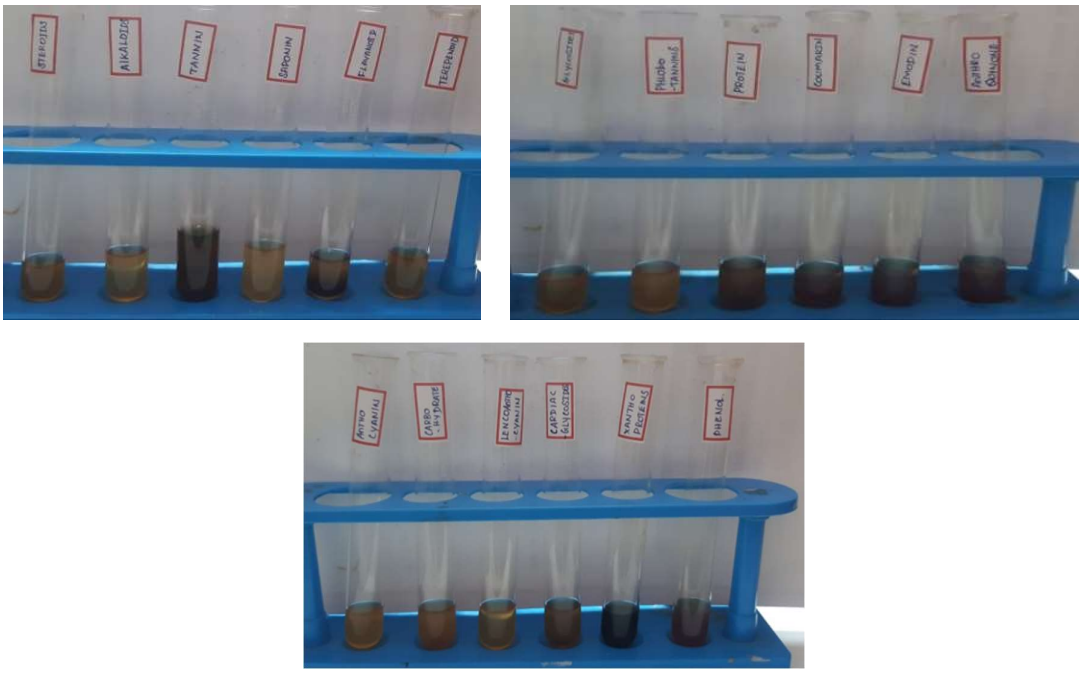


**Figure 2: Qualitative analysis of stem bark of *Hybantus enneaspermus***

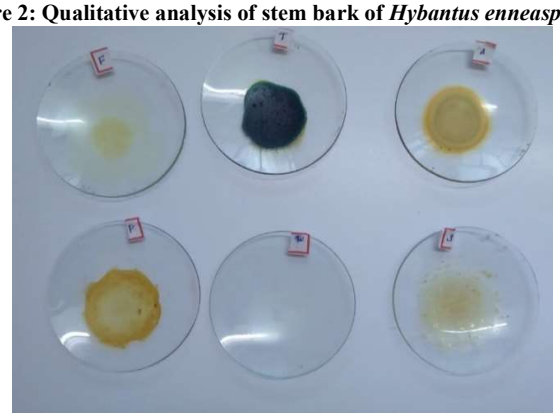

**Figure 3: Quantitative analysis of *Hybanthus enneaspermus* bark extract**

**Table 3: Quantitative analysis of stem bark of *Hybanthus enneaspermus***

| S. NO | Phytochemical constitutents | Stem bark of *Hybanthus enneaspermus* (mg/g) |
|---|---|---|
| 1 | Saponins | 0.018 |
| 2 | Alkaloids | 0.002 |
| 3 | Flavonoids | 0.004 |
| 4 | Phenols | 0.005 |
| 5 | Terpenoids | 0.004 |
| 6 | Tannins | 0.017 |

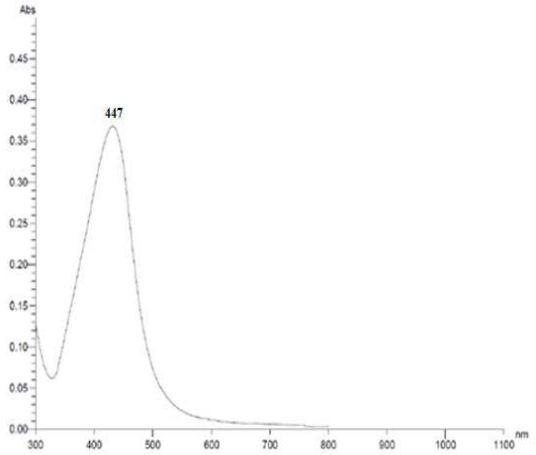


**Figure 4: UV-Vis spectrum of produced Ag Nps**

**Table: 4 FTIR band values of sample extract and synthesized silver nanoparticles**

| Functional group | Band | Frequency ($cm^{-1}$) |
|---|---|---|
| Primary amine | Strong band | 3331.07 agrees to broad N-H stretching amine |
| Isothiocyanate | Strong band | 1637.56 resembles to N=C=S stretching vibrations |
| Alkene | Medium band | 659.66 corresponds to C=C stretching conjugated alkene |
| Amine | Medium band | 597.93 resembles to O-H bending alcohol |
| Alcohol | Strong band | 557.43 agrees to C=O secondary alcohol |
| Anhydride | Strong band | 437.04 resembles to CO-O-CO anhydride |
| Halo compound | Strong band | 414.70 relates to C-Br stretching vibrations |

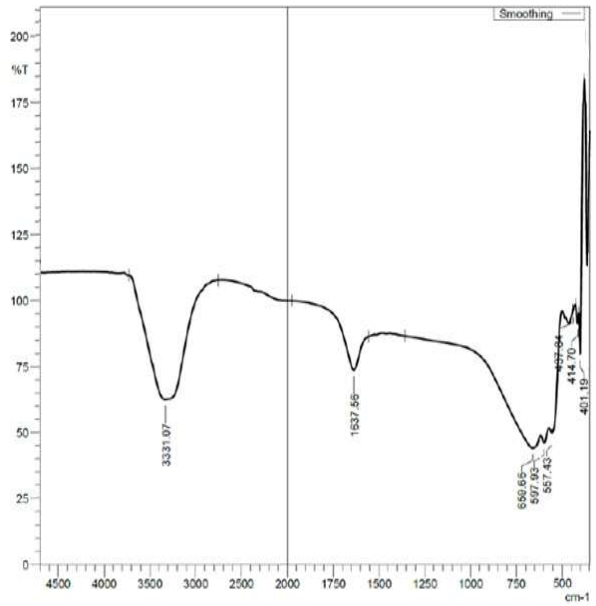


**Figure 5: FT-IR spectra of produced Ag Nps**

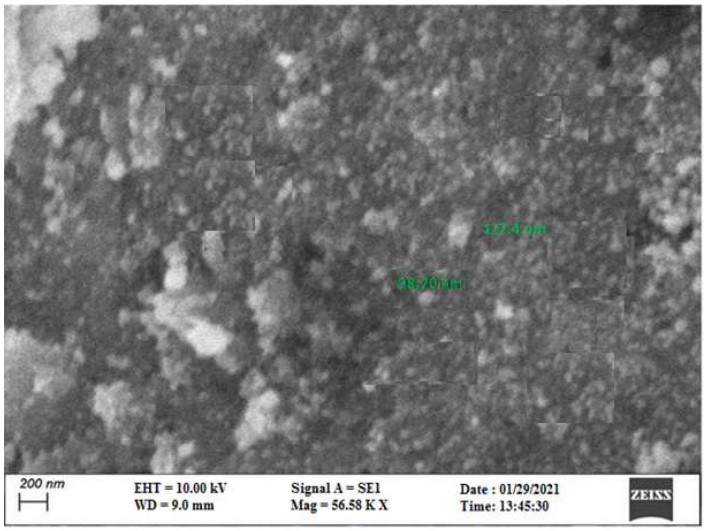


**Figure 6: SEM image for synthesized silver nanoparticles**

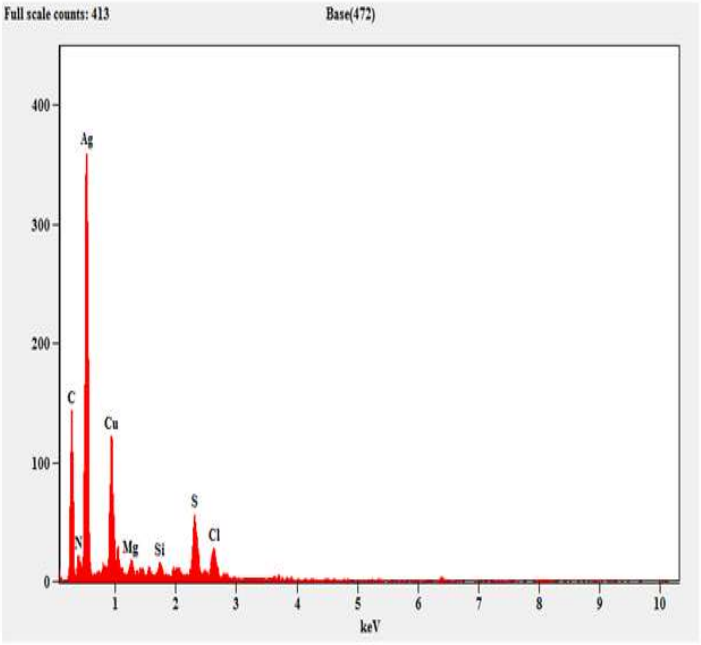


**Figure 7: EDX spectra of synthesized silver nanoparticles**

**Table 5: Elemental composition of synthesized silver nanoparticles**

| ELEMENT | WT% | AT% |
|---|---|---|
| C | 7.93 | 10.75 |
| N | 20.29 | 23.58 |
| Ag | 60.34 | 61.42 |
| Mg | 0.47 | 0.32 |
| Si | 0.42 | 0.24 |
| S K | 5.75 | 1.67 |
| Cl K | 1.06 | 0.49 |
| Cu K | 5.95 | 1.53 |
| Total | 100.00 | 100.00 |

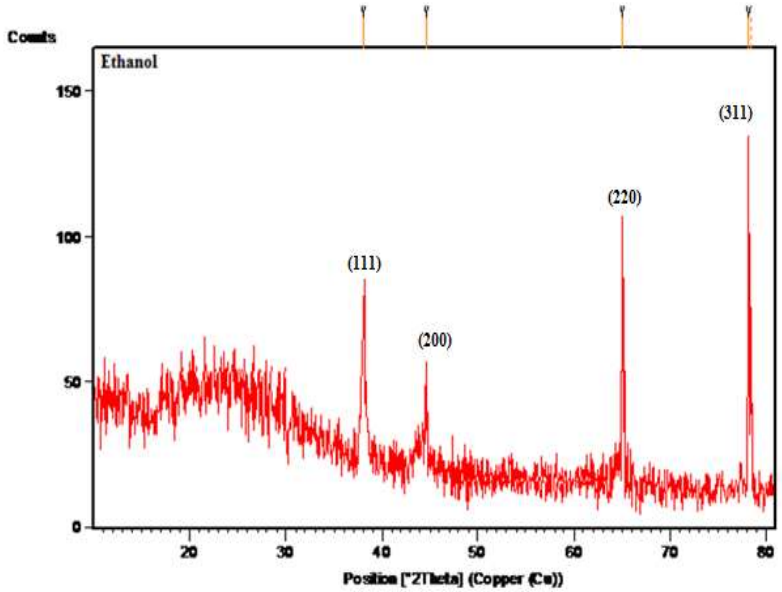


**Figure 8: XRD patterns of silver nanoparticles synthesized using a sample**

**Table 6: Harvested crystals percentage inhibition**

| Crystal | Class | Analysis | Harvested crystals (gm) | Inhibition Percentage |
|---|---|---|---|---|
| Struvite | A | Control | 2.46 | 0% |
| | B | Control +distilled water | 2.12 | 13.8% |
| | C | Control + ethanol solution | 1.48 | 39.8% |
| | D | Control + 1% synthesized silver nanoparticles | 1.26 | 48.7% |
| | E | Control + 2% synthesized silver nanoparticles | 0.85 | 65.4% |
| | F | Control + 3% synthesized silver nanoparticles | 0.69 | 71.9% |
| | G | Control + 4% synthesized silver nanoparticles | 0.47 | 80.8% |
| | H | Control + 5% synthesized silver nanoparticles | 0.25 | 89.8% |

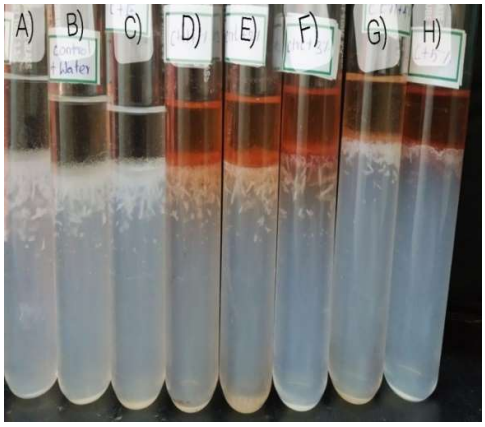


**Figure 9: Growth of CHPD**

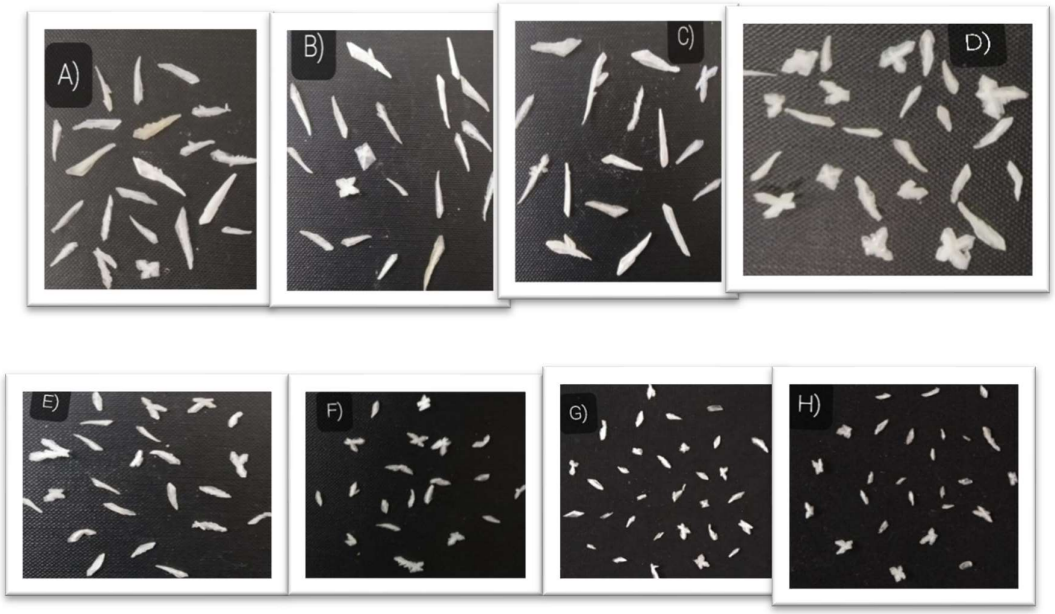


**Figure 10: Morphology of harvested CHPD crystals**

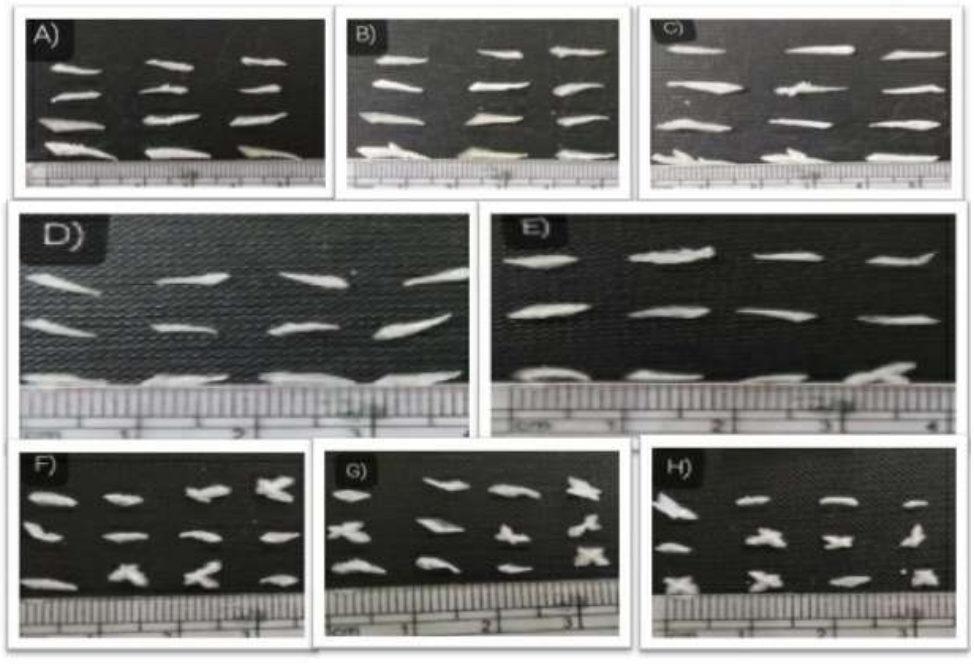


**Figure 11: Scale measurement of harvested of CHPD crystals**

**Table 7: FT-IR study of harvested crystals**

| Figure | Frequency $cm^{-1}$ | Functional group |
|---|---|---|
| Control A | 2358 | Anti-symmetric and symmetric stretching Vibration of $NH_4$ units |
| | 1636 | HOH deformation of water |
| | 1440 | HNH deformation of $NH_4$ units |
| | 1004 | V3 antisymmetric stretching vibration |
| | 758 | Liberation of water and $NH_4$ rocking modes |
| | 568 | V4 bending modes of the $PO_4$ units |
| Control+5% | 2374 | Antisymmetric and symmetric stretching, vibration of $NH_4$ units |
| | 1600 | HOH deformation of water |
| | 1438 | HNH deformation of modes of $NH_4$ units |
| | 1004 | V3 antisymmetric stretching vibration |
| | 758 | Liberation of water and $NH_4$ rocking modes |
| | 568 | V4 bending modes of the $PO_4$ units |

## CONCLUSION

Silver nanoparticles were created in this work using an ethanolic extract of *Hybanthus enneaspermus* stem bark. Terpenoids, flavonoids, tannins, alkaloids, steroids, coumarins, emodins, anthroquinones, phenols, and xanthoproteins were found in the phytochemical qualitative approach. The quantitative examination of phytoconstituents found that stem bark extract includes a high concentration of alkaloids, preceded with phenols, flavonoids, tannins, terpenoids, and saponins. The UV-Visible spectroscopy is utilized to characterize the produced Ag Nps, and the peak intensity is detected at 447nm. The existence of phytochemicals in the plant extract and the presence of functional groups under the characteristic of FTIR analysis confirms the development of Ag Nps. The cubic and spherical shapes of the produced Ag Nps were revealed by SEM examination. The presence of components in produced silver nanoparticles is verified by EDX analysis. The silver nanoparticles' crystalline nature is determined by XRD analysis. The antiurolithiatic activity was determined using the single gel diffusion technique. The findings revealed that silver nanoparticles mediated by *Hybanthus enneaspermus* are effective at controlling the formation of struvite kidney stones.

**Acknowledgment**

The authors thank to Chemistry Department, Holy Cross College, Thiruchirapalli, Tamilnadu, India, for providing necessary research facilities.

## REFERENCES

**[1]** P. Thuesombat, S. Hannongbua, S. Akasit and S. Chadchawan, *Ecotoxicol. Environ. Saf*. 104, 302 (2014). https://doi.org/10.1016/j.ecoenv.2014.03.022

**[2]** C. Larue, H. Castillo-Michel, S. Sobanska, L. Cecillon, S. Bureau

and V. Barthes, *J. Hazard. Mater*. 264, 98 (2014). https://doi.org/10.1016/j.jhazmat.2013.10.053

**[3]** G.A. El-Chaghaby and A.F. Ahmad, *Orient. J. Chem*. 27, 929 (2011).

**[4]** R. Veerasamy, T.Z. Xin, S. Gunasagaran, T.F.W. Xiang, E.F.C. Yang and N. Jeyakumar, *J. Saudi Chem. Soc*. 15, 113 (2011). https://doi.org/10.1016/j.jscs.2010.06.004

**[5]** M.R. Bindhu and M. Umadevi, *Spectrochim. Acta A*. 135, 373 (2015). https://doi.org/10.1016/j.saa.2014.07.045

**[6]** S. Mahdi, M. Taghdiri, V. Makari and M. Rahimi-Nasrabadi, *Spectrochim. Acta A*. 136, 1249 (2015). https://doi.org/10.1016/j.saa.2014.10.010

**[7]** H. Padalia, P. Moteriya and S. Chanda, *Arab. J. Chem*. 135, 373 (2014). http://dx.doi.org/10.1016/j.arabjc.2014.11.015.

**[8]** P.R.R. Sre, M. Reka, R. Poovazhagi, M.A. Kumar and K. Murugesan, *Spectrochim. Acta A*. 135, 1137 (2015). https://doi.org/10.1016/j.saa.2014.08.019

**[9]** S. Ahmed, M. Ahmad, B.L. Swami and S. Ikram, *J. Adv. Res*. 7, 17 (2016). http://dx.doi.org/10.1016/j.jare.2015.02.007

**[10]** S. Ahmed, M. Ahmad and S. Ikram, *J. Appl. Chem.* 3, 493 (2014).

**[11]** O.V. Kharissova, H.V.R. Dias, B.I. Kharisov, B.O. Perez and V.M.J. Perez, *Trends Biotechnol*. 31, 240 (2013). https://doi.org/10.1016/j.tibtech.2013.01.003

**[12]** J. Mittal, A. Batra, A. Singh and M.M. Sharma, *Adv. Nat. Sci.: Nanosci. Nanotechnol*. 5. (2014). http://dx.doi.org/10.1088/2043-6262/5/4/ 043002, 043002.

**[13]** B. Sadeghi and F. Gholamhoseinpoor, *Spectrochim. Acta A*. 134, 310 (2015). https://doi.org/10.1016/j.saa.2014.06.046

**[14]** S. Ashokkumar, S. Ravi and S. Velmurugan, Spectrochim. Acta Part A. 115, 388 (2013). https://doi.org/10.1016/j.saa.2013.06.050

**[15]** P. Logeswari, S. Silambarasan and J. Abraham, *Scientia Iranica.* 20, 1049 (2013).

**[16]** P. Logeswari, S. Silambarasan and J. Abraham, *J. Saud. Chem. Soc*. 19, 311 (2012).

**[17]** Z. Salari, F. Danafar, S. Dabaghi and S.A. Ataei, *J. Saud. Chem. Soc*. 20, 459 (2014). http://dx.doi.org/10.1016/j.jscs.2014.10.004.

**[18]** M.M.H. Khalil, E.H. Ismail, F. El-Magdoub, *Arab. J. Chem*. 5, 431 (2012). https://doi.org/10.1016/j.arabjc.2010.11.011

**[19]** C. Krishnaraj, E.G. Jagan, S. Rajasekar, P. Selvakumar, P.T. Kalaichelvan and N. Mohan, *Colloids Surfaces B.* 76, 50 (2010). https://doi.org/10.1016/j.colsurfb.2009.10.008

**[20]** A. Nabikhan, K. Kandasamy, A. Raj and N.M. Alikunhi, *Colloids Surfaces B*. 79, 488 (2010). https://doi.org/10.1016/j.colsurfb.2010.05.018

**[21]** M. Kifayatullah, H. Rahim, N.U. Jan, S. Abbas, M.S. Khan and M. Ikram, *Sains Malaysiana*, 48(5), 1075 (2019). http://dx.doi.org/10.17576/jsm-2019-4805-16

**[22]** J. Marcon, S. Schubert, C.G. Stief and G. Magistro, *Infection.* 1 (2019). https://doi.org/10.1007/s15010-019-01315-4

**[23]** A. Patle, K.V. Hatware, K. Patil, S. Sharma and G. Gupta, *J. Environ. Pathol. Toxicol. Oncol.* 38, 97 (2019). 10.1615/JEnvironPatholToxicolOncol.2019029075

**[24]** J. Jeevanandam, A. Barhoum, Y.S. Chan, A. Dufresne and M.K. Danquah, *Beilstein J. Nanotechnol*. 9, 1050 (2018). https://doi.org/10.3762/bjnano.9.98